

## AN SZ/X-RAY GALAXY CLUSTER MODEL AND THE X-RAY FOLLOW-UP OF THE PLANCK CLUSTERS

A. CHAMBALLU<sup>1,2</sup>, J. G. BARTLETT<sup>2</sup>, J.-B. MELIN<sup>3</sup>, M. ARNAUD<sup>4</sup>

<sup>1</sup> *Astrophysics group, Blackett Laboratory, Imperial College, Prince Consort road,  
London NW7 2AZ, England*

<sup>2</sup> *Laboratoire AstroParticule & Cosmologie (APC), Université Paris Diderot,  
10, rue Alice Domon et Léonie Duquet, 75205 Paris Cedex 13, France (UMR 7164)*

<sup>3</sup> *CEA, DSM, SPP, 91191 Gif sur Yvette, France*

<sup>4</sup> *CEA, DSM, SAp, 91191 Gif sur Yvette, France*

Sunyaev-Zel'dovich (SZ) cluster surveys will become an important cosmological tool over next few years, and it will be essential to relate these new surveys to cluster surveys in other wavebands. We present an empirical model of cluster SZ and X-ray observables constructed to address this question and to motivate, dimension and guide X-ray follow-up of SZ surveys. As an example application of the model, we discuss potential *XMM-Newton* follow-up of *Planck* clusters.

### 1 Introduction

Galaxy clusters are powerful cosmological probes: observations of their internal structure provide information on dark matter and can be used to estimate distances, while studies of their evolution gauge the influence of dark energy on structure formation – as rare objects at the top of the mass hierarchy, their number density and its evolution are extremely sensitive to the underlying cosmology. For these reasons, the Dark Energy Task Force included cluster surveys among the four primary methods for constraining dark energy. In this context, massive clusters are the most pertinent because their properties are little affected by non-gravitational processes.

Today, we do not yet have the large samples of clusters, most notably massive clusters, out to high redshifts (e.g. unity and beyond) needed to fully realize the potential of cluster studies. This is changing, thanks in large part to Sunyaev-Zel'dovich (SZ) cluster surveys. The SZ effect<sup>1,2,3</sup> is a distortion of the cosmic microwave background (CMB) black body spectrum due to inverse Compton scattering of CMB photons off electrons in the intra-cluster medium (ICM). It is one of the most promising ways of finding new galaxy clusters, since its amplitude (in terms of surface brightness) and spectrum are independent of redshift (in the non-relativistic case). As SZ surveys begin to open this new window on cluster science, relating them to surveys in other wavebands becomes a critical issue, both to understand what we are finding and to fully exploit their scientific potential.

### 2 An SZ/X-ray Cluster Model

Observations of the SZ effect give only two-dimensional information projected onto the sky, and follow-up in other wavebands is essential for most studies. Obviously, optical/NIR follow-up is

needed to obtain redshifts. Much can also be gained by combining X-ray and SZ data sets, for instance to better understand various survey selection functions. Follow-up with *XMM-Newton* and *Chandra* will enable us to probe the ICM with unprecedented precision, e.g. its thermal structure and the gas mass fraction. Moreover, with X-ray data we can estimate cluster masses through application of hydrostatic equilibrium.

In order to inform such SZ/X-ray comparisons and follow-up of SZ surveys, we have constructed an empirical and easily adaptable model<sup>4</sup> relating the SZ and X-ray properties of clusters. This section briefly summarizes its most relevant aspects.

### 2.1 Description of the model

Our model is based on several ingredients, derived from observations, numerical simulations and theory. We employ scaling laws in order to relate observed properties with the fundamental cluster parameters, mass and redshift: the  $M_{500} - T^{5,6}$ ,  $L_X - T^7$  and  $f_{gas} - T^8$  relations. The evolution of all these scaling relations is still poorly constrained. However, recent observations<sup>9,10</sup> indicate that self-similar evolution tends to reproduce well the data. Given this, we adopted self-similar evolution in all cases, and we subsequently validated this choice (see next section).

We approximate the spatial structure of the gas with an isothermal  $\beta$ -model<sup>a</sup> with  $\beta = 2/3$ . Fitting the  $L_X - T$  relation then requires a deviation from self-similarity in the  $f_{gas} - T$  relation, i.e., the gas mass fraction varies with cluster total mass; this variation is allowed by present observations. For the dark matter, we adopt a NFW profile and use the Jenkins mass function<sup>12</sup>. Local cluster counts in terms of the X-ray Temperature Function<sup>11</sup> (XTF) then fix the normalization of the fluctuation power spectrum (using the measured  $M_{500} - T$ ).

By combining these different ingredients we constrain all free parameters of the model, namely those describing cluster physics – like the core radius  $r_c$  and the central electronic density  $n_e$  – and those describing population statistics, such as  $\sigma_8$  (see below). We took particular care with the various mass definitions available in the literature, related to theoretical studies (e.g.  $M_{vir}$ ), observations (e.g.  $M_{500}$ ) or numerical simulations (e.g. masses estimated by the friends-of-friends method), transforming among them with the NFW dark matter profile. This was indispensable for coherently combining the variety of constraints.

### 2.2 Model validation

To validate the model, we checked it against additional observational constraints, not used to fix its parameters. We discuss below the most relevant of these, but cite another notable one in passing: fitting the local XTF<sup>11</sup> we find  $\sigma_8 = 0.78 \pm 0.027$ , in complete agreement with WMAP-5 results<sup>15</sup>. More specifically, we tested the model by comparing the observed redshift distributions from the REFLEX<sup>13</sup> and 400 square-degree<sup>14</sup> surveys to the predictions of the model. Figure 1 shows the predicted and observed counts in both cases. In the former case, the observed total number of clusters is 447 with a completeness estimated to be at least 90%; the predicted number is 508 clusters, which corresponds to 457 clusters for a completeness of 90%. Moreover, the shapes of the two distributions are in very good agreement.

In the case of the 400deg<sup>2</sup> survey, the model reproduces extremely well the high redshift distribution ( $z > 0.4$ ), although it seems to predict too many low redshift clusters. Noting that this is a serendipitous survey, in which known local clusters are by construction missing, we conclude once again that the model is in reasonable agreement with the data. This last result is particularly satisfying since the high redshift clusters contained in this deep survey are of the kind expected to be found in SZ surveys like *Planck* (as discussed below).

<sup>a</sup>This will be improved in a future version of the model, to account for recent observations showing that this profile is inadequate, especially in the core and outer parts of clusters.

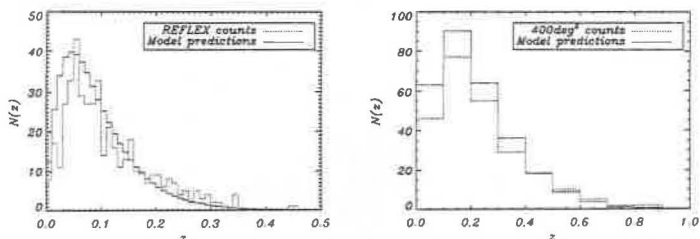


Figure 1: Two examples of the redshift distribution of clusters from ROSAT surveys (red) compared to model predictions (blue). *Left:* The REFLEX survey. *Right:* The 400 square-degree survey.

### 3 An application of the model

The model is completely general and can be used to predict the results of any set of SZ and X-ray observations. As an example of its application, we discuss potential follow-up of *Planck* SZ clusters with *XMM-Newton*.

#### 3.1 The *Planck* cluster catalog

To accurately model the *Planck* cluster catalog, we employed the selection function derived using the detection algorithms developed by Melin et al.<sup>16</sup> and applied to detailed simulations of *Planck* observations (the *Planck* Sky Model<sup>17</sup>). We find that a non-negligible fraction of otherwise bright SZ clusters remain undetected: these are resolved, low to intermediate redshift clusters whose SZ flux is diluted over several pixels. This selection effect is shown in the left-hand panel of Figure 2, where we plot the cumulative redshift distribution of *Planck* clusters.

The result is that the *Planck* catalog is expected to contain  $\sim 2350$  clusters, of which  $\sim 180$  are at  $z > 0.6$  and  $\sim 15$  at  $z > 1$ ; there is, of course, a certain amount of model uncertainty associated with these predictions, in particular from the normalization of the SZ-mass relation.

#### 3.2 Follow-up with *XMM-Newton*

We wish to identify the X-ray nature of these new *Planck* clusters and evaluate the ability of *XMM-Newton* to observe a significant number of them. We therefore examine those clusters with X-ray fluxes below the ROSAT All Sky Survey (RASS) limit, which we take to be  $f_X [0.1 - 2.4] \text{keV} = 10^{-12} \text{ erg s}^{-1} \text{ cm}^{-2}$  (i.e., the lowest limit of the MACS survey<sup>18</sup>). The distribution of this sub-catalog of new *Planck* clusters is given as a function of redshift and predicted temperature in the central panel of Figure 2. Most of the ( $\sim 520$ ) clusters are relatively cool and local; however,  $\sim 168$  clusters lie at  $z > 0.6$  and have temperatures  $T > 6 \text{keV}$ . Note that only six such clusters are presently known.

In the right-hand panel of Figure 2, we show the expected X-ray flux of these objects in the *XMM-Newton* [0.5-2]-keV band as contours projected onto the redshift-temperature plane. This allows us to evaluate their detectability, and we see that all of these *Planck* clusters have fluxes larger than  $10^{-13} \text{ erg s}^{-1} \text{ cm}^{-2}$ . They are bright, falling in the flux decade just below the ROSAT limit. This has important consequences for follow-up programs.

Using observations of MS1054-0321<sup>19</sup> and ClJ1226.9+3332<sup>20</sup> - two clusters of the same kind as the newly-discovered high redshift *Planck* clusters - as a guide, we estimate that *XMM-Newton* could measure the temperature of *Planck* clusters at  $z > 0.6$  to 10% with a relatively

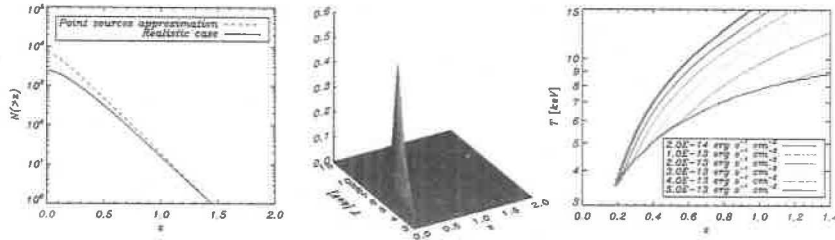


Figure 2: *Left*: Predicted cumulative redshift distribution of the *Planck* cluster catalog. The dashed red line corresponds to the case where all clusters are (falsely) imagined to be unresolved (point-source approximation); the blue line is the realistic case, accounting for the fact that some clusters are resolved. *Middle*: The *Planck* newly-discovered cluster catalog (in which clusters are observed by *Planck* but not by ROSAT) distributed in bins over temperature and redshift. *Right*: The same distribution projected over the  $(z, T)$ -plane with contours of iso-flux in the *XMM-Newton* [0.5-2]-keV band.

short exposure of 25-50 ks (per cluster). It should also be possible to obtain masses and mass profiles for the reasonably relaxed clusters by applying hydrodynamic equilibrium equation.

#### 4 Summary

We presented a model for the SZ and X-ray signals of galaxy clusters based on current X-ray data. Using a realistic mock *Planck* cluster catalog, we employed the model to predict, firstly, that  $\sim 168$  newly-discovered clusters lie at  $z > 0.6$  with  $T > 6\text{keV}$ , and secondly, that these clusters can be observed in some detail in only 25-50 ks with *XMM-Newton*. Thus we could follow-up the majority of these new *Planck* clusters with a dedicated program of several Msec on *XMM-Newton*; this falls in the category of *Very Large Programme* now possible with the satellite. Follow-up observations with *XMM-Newton* would therefore dramatically increase the sample of well-studied, massive, high redshift ( $0.6 < z < 1$ ) clusters, key objects for precise cosmology with clusters and for testing gravitational processes in cluster formation.

#### References

1. R. A. Sunyaev & Y. B. Zel'dovich, *Comments on Astrophysics and Space Physics* 4, 173 (1972)
2. M. Birkinshaw, *Phys. Rep.* 310, 97 (1999)
3. J. E. Carlstrom, G. P. Holder & E. D. Reese, *ARA&A* 40, 643 (2002)
4. A. Chamballu, J. G. Bartlett, J.-B. Melin & M. Arnaud, *in preparation* (2008)
5. M. Arnaud, E. Pointecouteau & G. W. Pratt, *A&A* 441, 893 (2005)
6. A. Vikhlinin, A. Kravtsov, W. Forman et al., *ApJ* 640, 691 (2006)
7. M. Arnaud & G. E. Evrard *MNRAS* 305, 631 (1999)
8. J. J. Mohr, B. Mathiesen & A. E. Evrard, *ApJ* 517, 627 (1999)
9. O. Kotov & A. Vikhlinin, *ApJ* 641, 752 (2006)
10. F. Pacaud, M. Pierre, C. Adami et al., *MNRAS* 382, 1289 (2007)
11. J. P. Henry, *ApJ* 609, 603 (2004)
12. A. Jenkins, C. S. Fraix, S. D. M. White et al., *MNRAS* 321, 372 (2001)
13. H. Böhringer et al., *A&A* 425, 367 (2004)
14. R. A. Burenin et al., *ApJS* 172, 561 (2006)
15. J. Dunkley, E. Komatsu, M. R.olta et al., *ArXiv e-prints* (2008)
16. J. B. Melin, J. G. Bartlett & J. Delabrouille, *A&A* 459, 341 (2006)
17. [http://www.apc.univ-paris7.fr/APC\\_CS/Recherche/Adamis/PSM/paky-en.html](http://www.apc.univ-paris7.fr/APC_CS/Recherche/Adamis/PSM/paky-en.html)
18. H. Ebeling, A. C. Edge & J. P. Henry, *ApJ* 553, 668 (2001)
19. I. M. Gioia, V. Braito, M. Branchesi et al., *A&A* 419, 517 (2004)
20. B. J. Maughan, C. Jones, L. R. Jones & L. Van Speybroeck, *ApJ* 659, 1125 (2007)